A Photonic Microwave Filter Based on an Asymmetric Silicon Mach-Zehnder Modulator
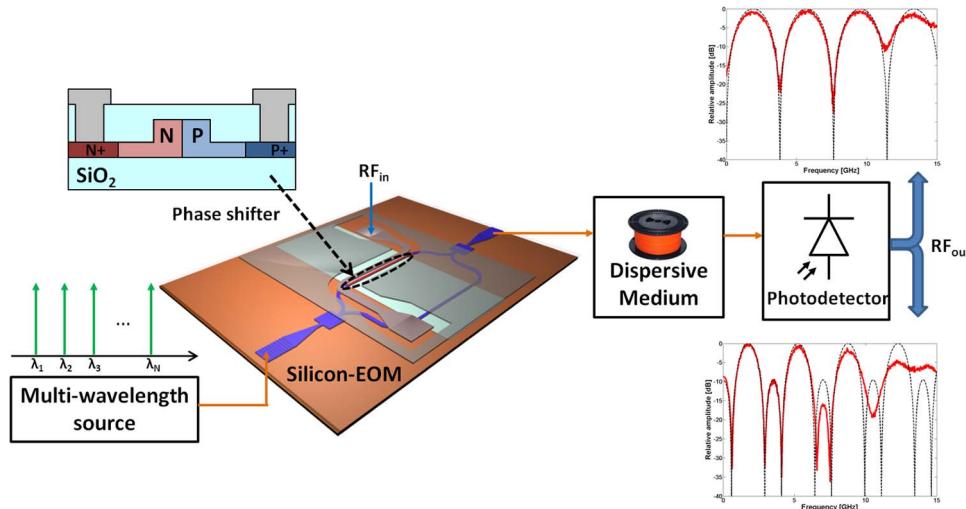
A. M. Gutiérrez
P. Sanchis
A. Brimont
D. J. Thomson
F. Y. Gardes
G. T. Reed
J.-M. Fedeli
B. Vidal

A Photonic Microwave Filter Based on an Asymmetric Silicon Mach-Zehnder Modulator

A. M. Gutiérrez,[1] **P. Sanchis,**[1] **A. Brimont,**[1] **D. J. Thomson,**[2] **F. Y. Gardes,**[2] **G. T. Reed,**[2] **J.-M. Fedeli,**[3] **and B. Vidal**[1]

[1]Nanophotonics Technology Center, Universitat Politecnica Valencia, 46022 Valencia, Spain
[2]Optoelectronics Research Centre, University of Southampton, Southampton SO17 1BJ, U. K.
[3]CEA, LETI, 38054 Grenoble Cedex, France

Abstract: A new approach for implementing an integrable photonic microwave filter based on exploiting the asymmetry of a CMOS-compatible silicon Mach-Zehnder modulator is demonstrated. The strong dependence of the modulator response with wavelength is exploited for achieving positive and negative taps and, therefore, a fully reconfigurable filter, without the complexity of previous approaches. Two filter responses with two and three taps are experimentally demonstrated, showing the proof-of-principle for frequencies up to 10 GHz and thus going one step further toward a full integration of the complete filter device in the CMOS-compatible silicon photonics platform.

Index Terms: Integrated optics, microwave photonics, modulators, silicon photonics, fiber optics and optical communications.

1. Introduction

The use of optical fiber in microwave applications offers an unmatched alternative in terms of time-bandwidth product, loss per meter, flexibility, and electromagnetic immunity when compared to conventional microwave implementations. In addition to the transmission of microwave signals, photonic technology can implement processing functionalities such as filtering with tuning and reshaping capabilities [1]–[4]. However, the competitiveness of these filters is constrained by the cost, size, and power consumption of microwave photonics solutions based on discrete components. Photonic integrated circuits (PIC) directly address these issues and are a promising path to broaden the applicability of microwave photonics [5].

Several photonic integrated devices for microwave applications have been recently reported, such as coherent notch [6], [7] and pass-band [8] filters, phase tuning in incoherent filters [9], beamforming [5], RF mixer [10], modulation enhancement in analog links [10], or an integrated dispersive element [12]. Among the different technologies, silicon photonics is currently one of the most promising CMOS-compatible platforms for enabling large scale photonic integration together with electronics [13].
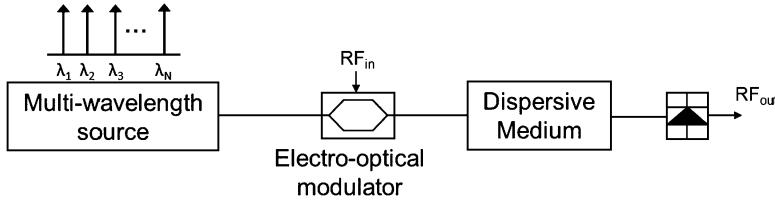
Fig. 1. Block diagram of the dispersion-based photonic microwave filter.

The proposed photonic microwave filter is based on an asymmetric silicon Mach-Zehnder modulator (MZM). The asymmetry, which is achieved by introducing a length difference between the MZM arms, is used to obtain positive and negative taps at the 1550 nm wavelength band (C-band) thanks to the associated strong wavelength dependence of the modulator response in combination with the π-phase inversion after photo-detection. Bipolar filter taps allow the implementation of a wide range of filter responses without the limitations of pure positive designs while keeping the inherent stability of incoherent operation. Unlike previous proposals using a single modulator [15], the proposed technique avoids the need of combined 1300 nm and 1550 nm optical sources. Therefore, the new approach simplifies the filter architecture and allows its use with erbium-doped fiber amplifiers (EDFAs) as well as integrated dispersive delay lines (such as [12]) which can lead to the development of fully integrated photonic microwave filters.

2. Photonic Microwave Filter Architecture

Fig. 1 shows the block diagram of the proposed dispersion-based photonic microwave filter. This filter architecture is well-known for optical processing of radio-frequency (RF) signals. The principle of operation is based on modulating a multi-wavelength optical source with the input microwave signal (RF_{in}). The modulated signal is then propagated through a dispersive medium and photo-detected to obtain the filtered microwave signal (RF_{out}). Hence, each optical source implements a filter sample that is selectively delayed by employing the dispersive medium. The amplitude of each sample can be changed by using different techniques, but the simplest way is controlling the output power of the optical sources. In such a way, a finite impulse response (FIR) filter can be implemented with transfer function expressed as

$$H(\omega) = \sum_{n=0}^{N-1} a_n e^{-jn\omega T} \tag{1}$$

where the number of filter coefficients, N, is determined by the number of optical wavelengths; the amplitude of each coefficient, a_n, is controlled with the optical power of each wavelength; and the time delay, T, depends on the dispersion of the dispersive medium.

The main advantage of this filter architecture is a very stable response due to operation in the incoherent regime. Furthermore, the filter transfer function can be reconfigured by dynamically changing the relative power of the optical wavelengths, and it can be tuned by controlling the dispersive medium [1]. However, positive and negative filter coefficients are needed to allow a full versatility in the transfer function, thus enabling flat-pass bands or high out-of-band suppression [14], [15]. The equivalent of positive and negative coefficients can be obtained by using opposite slopes of the modulation transmission response [14]. In this way, positive and negative coefficients for a FIR filter can be obtained while keeping the stability inherent to incoherent operation. This technique has been employed with only one single LiNbO$_3$ MZM, as shown in Fig. 1, by exploiting the V_π dependence with wavelength [15]. However, this dependence was very weak, and optical sources with a very large separation (1300 and 1550 nm) were required. That makes the filter implementation complex, introduces high loss at 1300 nm (more than 20 dB) since the modulator is
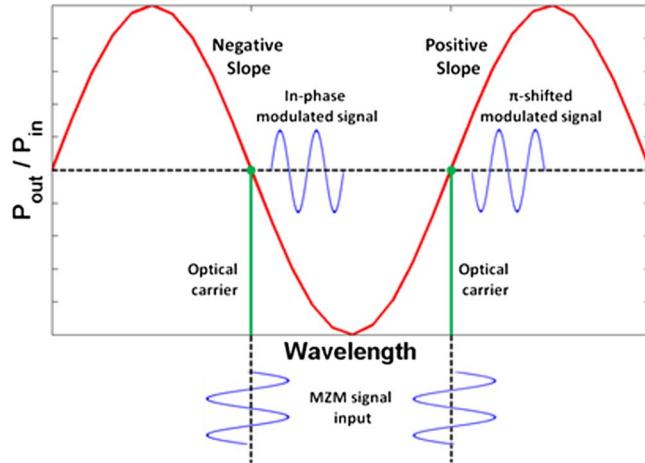
Fig. 2. Concept of the π phase inversion experienced by two microwave modulating signals.
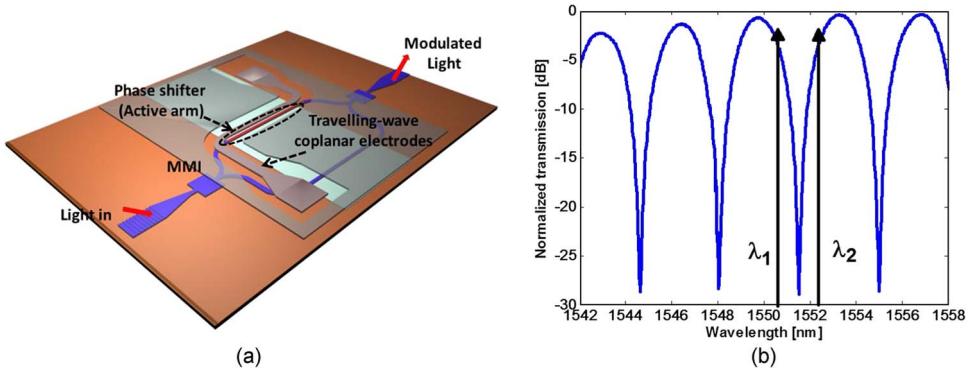

Fig. 3. (a) Schematic of the silicon Mach-Zehnder modulator for implementing the photonic microwave filter. (b) Measured modulator transmission response for a fixed 4 V applied DC voltage.

not optimized for operation at both 1550 and 1300 nm, prevents the use of EDFAs, and limits further integration with other subsystems such as on-a-chip dispersive delay lines [12].

In this work, we propose a new approach for achieving positive and negative coefficients based on exploiting the asymmetry of a silicon MZM. The principle of operation is more clearly depicted in Fig. 2. The MZM asymmetry introduces a strong dependence with wavelength in the modulator transmission response. Therefore, if, for instance, two optical carriers modulated by a microwave signal are placed at wavelengths that correspond with opposite slopes in the MZM response, the microwave signals obtained after photodetection will have the same average power but inverted phase (i.e., π-shifted). Linearity must be ensured by placing the optical carriers at the quadrature bias point of the modulator response, as shown in Fig. 2. The effect of drifts in the optical carrier amplitude and wavelength is translated in a residual sidelobe level in the filter response [16].

The modulator, depicted in Fig. 3(a), was fabricated with standard CMOS fabrication steps [17]. The asymmetry of the modulator is achieved by introducing a length difference of only 180 μm between the MZM arms. Active performance is based on a reverse biased PN junction located in the middle of the optical waveguide and embedded in the shorter arm of the MZM. Multimode interference (MMI) couplers are used for splitting and combining the light in the MZM, as shown in
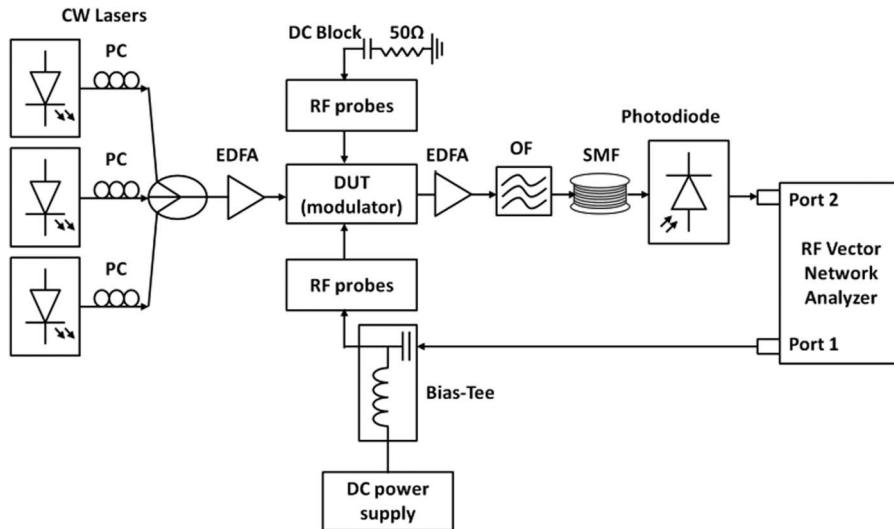
Fig. 4. Experimental setup for a three-tap photonic microwave filter architecture.

Fig. 3(a). Furthermore, a traveling-wave ground–signal–ground (GSG) coplanar design for the electrodes was used for maximizing the modulator bandwidth.

Fig. 3(b) shows the measured normalized transmission response of the MZM for a fixed 4 V applied DC voltage. The $V_\pi L_\pi$ product was estimated to be around 2.25 V · cm. On the other hand, the insertion loss of the MZM was around 12 dB though a large static extinction ratio close to 30 dB was measured, as it can be seen in Fig. 3(b).

3. Experimental Results

The experimental setup is shown in Fig. 4. A set of optical continuous wave (CW) carriers are modulated by the silicon MZM. The RF signal from a vector network analyzer (Agilent PNA-X) is combined with the DC voltage using a bias-Tee and applied to the modulator through a broadband GSG probe. The output of the electrode is terminated by a DC-block and a 50 Ω load using another GSG probe.

By choosing the wavelength of the optical carriers, it is possible to control the sign of the corresponding filter coefficient. After modulation, the signals are amplified with an EDFA, filtered by a tunable optical filter (OF), and launched to a dispersive medium (a reel of 10 km of single-mode fiber). Then, the optical signal is photo-detected and injected into the vector network analyzer. The dispersion in the reel of 10 km of single-mode fiber was first characterized as a function of wavelength with an optical network analyzer for allowing the comparison of experimental results with the theoretical transfer function described by eq. (1).

Fig. 5 shows the normalized filter response between 0-15 GHz when two optical carriers ($\lambda_1 = 1550.75$ nm and $\lambda_2 = 1552.30$ nm) enter the modulator with the same output power at the input of the photodiode. These wavelengths are placed at opposite slopes of the modulator response, as shown in Fig. 3(b), resulting in filter coefficients $[a_1\ a_2] = [-1\ 1]$. A very good agreement between theory and measurements can be seen in Fig. 5, demonstrating that two coefficients of opposite sign have been obtained.

Fig. 6 shows the filter response when three optical carriers (1547.51, 1549.13, and 1550.75 nm) are fed to the modulator. The filter response agrees again very well with the theoretical response corresponding to the amplitude distribution $[a_1\ a_2\ a_3] = [1\ -1\ 1]$ for frequencies up to 10 GHz. At higher frequencies, the agreement is reduced due to an unbalance in the modulation efficiency between optical carriers and the higher accuracy needed in time-delay among taps. Any distribution
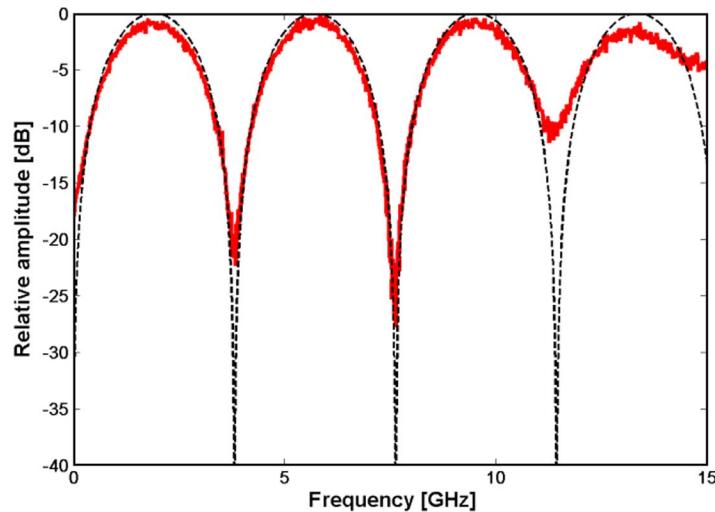
Fig. 5. Experimental two-tap filter response with amplitude distribution [1 −1]. The solid line represents the experimental results and the dotted the theoretical estimation.
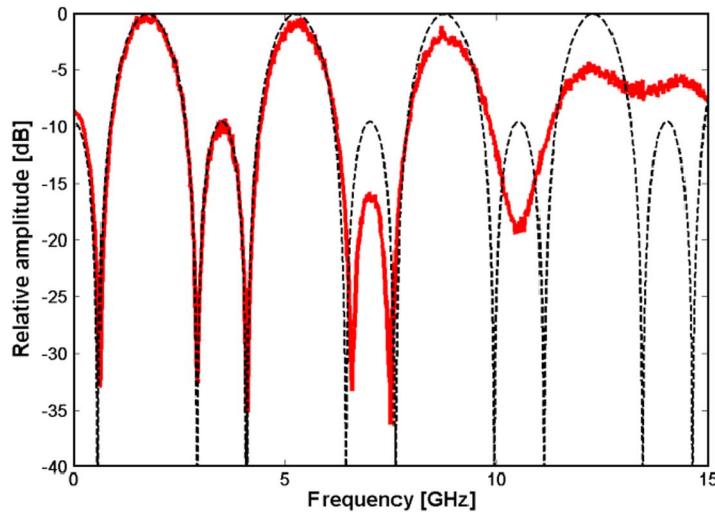

Fig. 6. Experimental three-tap filter response with amplitude distribution [1 −1 1]. The solid line represents the experimental results and the dotted the theoretical estimation.

of positive and negative coefficients can be implemented by using a pair of broadband OFs and time matching [15].

4. Conclusion

In conclusion, a novel photonic microwave filter implementation based on an asymmetric silicon MZM has been demonstrated. The asymmetry of the modulator structure has been exploited to achieve positive and negative filter coefficients at the 1550 nm wavelength band. Furthermore, the obtained results show the capability of the silicon photonics platform not only to open up the path to full integration of photonic microwave filters in a chip scale but also to enable the implementation of advanced functionalities.

References

[1] B. Vidal, V. Polo, J. L. Corral, and J. Martí, "Photonic microwave filter with tuning and reconfiguration capabilities using optical switches and dispersive media," *Electron. Lett.*, vol. 39, no. 6, pp. 547–549, Mar. 20, 2003.

[2] B. Vidal, T. Mengual, C. Ibáñez-López, and J. Martí, "WDM photonic microwave filter with variable cosine windowing based on a DGD module," *IEEE Photon. Technol. Lett.*, vol. 18, no. 21, pp. 2272–2274, Nov. 2006.

[3] E. H. W. Chan and R. A. Minasian, "Novel coherence-free RF/microwave photonic bandpass filter," *IEEE Photon. Technol. Lett.*, vol. 21, no. 4, pp. 230–232, Feb. 2009.

[4] V. R. Supradeepa, C. M. Long, R. Wu, F. Ferdous, E. Hamidi, D. E. Leaird, and A. M. Weiner, "Comb-based radio-frequency photonic filters with rapid tunability and high selectivity," *Nature Photon.*, vol. 6, no. 3, pp. 186–194, 2012.

[5] D. Marpaung, C. Roeloffzen, R. Heideman, A. Leinse, S. Sales, and J. Capmany, "Integrated microwave photonics," *Laser Photon. Rev.*, pp. 1–33, 2013.

[6] M. S. Rasras, K. Y. Tu, D. M. Gill, Y. K. Chen, A. E. White, S. S. Patel, A. Pomerene, D. Carothers, J. Beattie, M. Beals, J. Michel, and L. C. Kimerling, "Demonstration of a tunable microwave-photonic notch filter using low-loss silicon ring resonators," *J. Lightw. Technol.*, vol. 27, no. 12, pp. 2105–2110, Jun. 2009.

[7] J. Dong, L. Liu, D. Gao, Y. Yu, A. Zheng, T. Yang, and X. Zhang, "Compact notch microwave photonic filters using on-chip integrated microring resonators," *IEEE Photon. J.*, vol. 5, no. 2, p. 5500307, Apr. 2013.

[8] J. Palací, G. E. Villanueva, J. V. Galán, J. Martí, and B. Vidal, "Single bandpass photonic microwave filter based on a notch ring resonator," *IEEE Photon. Technol. Lett.*, vol. 22, no. 17, pp. 1276–1278, Sep. 2010.

[9] J. Lloret, J. Sancho, M. Pu, I. Gasulla, K. Yvind, S. Sales, and J. Capmany, "Tunable complex-valued multi-tap microwave photonic filter based on single silicon-on-insulator microring resonator," *Opt. Exp.*, vol. 19, no. 13, pp. 12402–12407, Jun. 2011.

[10] A. M. Gutiérrez, A. Brimont, J. Herrera, M. Aamer, J. Martí, D. J. Thomson, F. Y. Gardes, G. T. Reed, J. M. Fedeli, and P. Sanchis, "Silicon slow-light-based photonic mixer for microwave-frequency conversion applications," *Opt. Lett.*, vol. 37, no. 10, pp. 1721–1723, May 2012.

[11] A. Perentos, F. Cuesta-Soto, A. Canciamilla, B. Vidal, L. Pierno, N. S. Losilla, F. López-Royo, A. Melloni, and S. Iezekiel, "Using aSi$_3$N4 ring resonator notch filter for optical carrier reduction and modulation depth enhancement in radio-over-fiber links," *IEEE Photon. J.*, vol. 5, no. 1, p. 5500110, Feb. 2013.

[12] J. Sancho, J. Bourderionnet, J. Lloret, S. Combrié, I. Gasulla, S. Xavier, S. Sales, P. Colman, G. Lehoucq, D. Dolfi, J. Capmany, and A. De Rossi, "Integrable microwave filter based on a photonic crystal delay line," *Nature Commun.*, vol. 3, p. 1075, 2012.

[13] M. Hochberg, N. C. Harris, R. Ding, Y. Zhang, A. Novack, Z. Xuan, and T. Baehr-Jones, "Silicon photonics: The next fabless semiconductor industry," *IEEE Solid-State Circuits Mag.*, vol. 5, no. 1, pp. 48–58, Mar. 2013.

[14] J. Capmany, D. Pastor, A. Martinez, B. Ortega, and S. Sales, "Microwave photonic filters with negative coefficients based on phase inversion in an electro-optic modulator," *Opt. Lett.*, vol. 28, no. 16, pp. 1415–1417, Aug. 2003.

[15] B. Vidal, J. L. Corral, and J. Martí, "All-optical WDM multi-tap microwave filter with flat bandpass," *Opt. Exp.*, vol. 14, no. 2, pp. 581–586, Jan. 23, 2006.

[16] B. Vidal, J. L. Corral, and J. Martí, "Statistical analysis of WDM photonic microwave filters with random errors," *IEEE Trans. Microw. Theory Techn.*, vol. 53, no. 8, pp. 2600–2603, Aug. 2005.

[17] A. Brimont, A. M. Gutierrez, M. Aamer, D. J. Thomson, F. Y. Gardes, J. Fedeli, G. T. Reed, J. Marti, and P. Sanchis, "Slow-light-enhanced silicon optical modulators under low-drive-voltage operation," *IEEE Photon. J.*, vol. 4, no. 5, pp. 1306–1315, Oct. 2012.